Managing the Interdisciplinary Requirements of 3D Geological Models

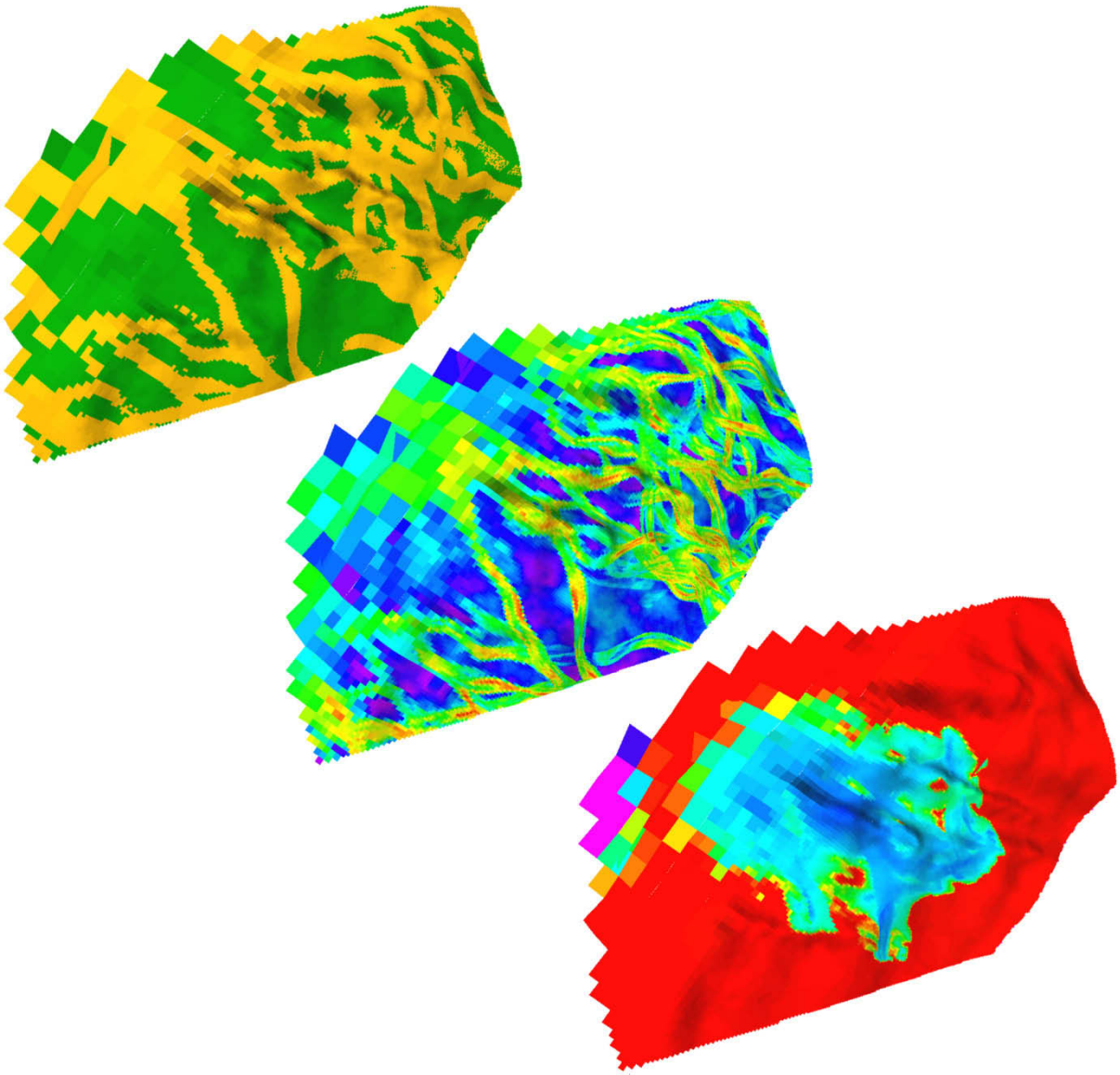

Sarah Jane Riordan
Australian School of Petroleum
University of Adelaide

March 2009

Thesis submitted in accordance with the requirements of the University of Adelaide

for the degree of Doctor in Philosophy

5 UPSCALING

When the static grids were upscaled they were analysed so that the changes that upscaling induced in the models could be understood. This chapter presents the results of the grid analysis and examines how cell dimensions influence the properties of static models as they are upscaled.

3D geological or static models are frequently upscaled prior to reservoir simulation. A variety of different methods are used, depending on the parameter in question. Facies models are usually upscaled by assigning the most frequent facies in the contributing cells to the upscaled cell (Roxar, 2006) and porosity is generally upscaled by calculating the arithmetic average of the contributing cells (Begg et al., 1996). There are many methods for upscaling permeability models for reservoir simulation. Summaries of the methods include Pickup et al. (1994b), Christie (1996), Renard and de Marsily (1997), and Durlofsky (2003).

5.1 Methodology

The base grids were upscaled vertically and horizontally. Vertical upscaling steps were two, three and four times (24 layers to 12 layers, 6 layers, 3 layers). The horizontal upscale steps used are 2, 4, 5, 10, 20, 40, 50 and 100 times (e.g. 1000 x 800 cells to 500 x 400 cells, 250 x 200 cells and so on). The number of rows and columns varies for each grid design). The dimensions of the cells in the grids can be seen in Figure 5.1 while Figure 5.2 shows the number of active cells associated with all the grids built and simulated.

Upscaling was carried out in RMS, using the ‘rescale’ module (Roxar, 2006). The entire grid was upscaled evenly with no editing of the grids around the wellbores. Facies models were upscaled using RMS’s ‘discrete’ upscaling, which assigns the most common facies in the contributing cells to the upscaled cell (Roxar, 2006). Porosity was upscaled using an

arithmetic average. The method used to upscale permeability in this project was the diagonal tensor method (Leung, 1986; Kasap and Lake, 1990; Mansoori, 1994; Pickup et al., 1994c).

The same permeability grid was used to generate horizontal permeability in the x and y directions (kx and ky) and vertical permeability (kz). Flow boundaries between all cells were open.

Ten realizations were generated for each scenario, in each grid design. Realizations 1–3 were upscaled vertically to 12, 6 and 3 layers and horizontally to all horizontal upscale steps (Figure 5.1). Realizations 4–10 were upscaled only to 3 layers, but to all horizontal upscale steps.

5.2 Results of Upscaling the Models

5.2.1 Facies Models

5.2.1.1 Channel Models

The channel models consist of two facies—channel and overbank. The channels were modelled as channel belts that have low sinuosity. A specific crevasse splay facies was not modelled. In the Flounder dataset, thin sands that were interpreted as crevasse splays, were assigned to the overbank facies. Thus the overbank facies porosity set will contain some potential reservoir quality values (see *section 5.2.2* for detailed discussion of porosity distribution).

The channel belts are distributed randomly across the field and vertically through the section. The channels have a mean thickness of 5 m, with a standard deviation of 1, resulting in a thickness range of 2–8 m. The average thickness of the cells in the models is 0.5 m in the 24-layer grids, 1 m in the 12-layer grids, 2 m in the 6-layer grid and 4 m in the 3-layer grid. Thus, the average channel thickness should be less that than the average cell thickness in the 3-layer grids (Figure 5.3).

The shape of the cells influences the preservation of channel morphology during the upscaling process. The square grid and the SDA grid, which has its long axis parallel to the channel orientation, preserve the channel morphology best in the upscaled cells (Figure 5.4, Figure 5.5, Figure 5.6 and Figure 5.7). Once the channel width is exceeded by the cell width, the width of the channels, where they are preserved, is controlled by the cell width—which may differ greatly from the original model input.

5.2.1.2 Coastal Models

The purpose of building a beach as well as a coast scenario was to establish how much, if any, influence on reservoir simulation results the presence of channels appear to have. More importantly, is the width of the channels a limiting factor in the upscaled model? The results of reservoir simulation of both scenarios are compared in *section 6.3.3* to establish if the influence of the channels could be identified in the cumulative production of the field.

In the facies models the interaction between grid orientation, cell shape and facies body shape is highlighted in the 'coast' scenario. This scenario contains two different depositional elements that are orientated at approximately right angles to each other. The influence of grid design on the results of upscaling facies and petrophysical models is highlighted in Figure 5.8 and Figure 5.9. Differences in grid design are not apparent in the base models. As the models are upscaled the influence of cell shape and the preservation of facies morphology become visible. Even when the cells are still smaller than the width of the fluvial channels (upscaled 10x), the morphology of the channels and of the coast/offshore interface is beginning to be influenced by cell shape (Figure 5.10). The square grid model retains the most detail of all the facies. It is also the best design for preserving the position of the shoreface during vertical upscaling (Figure 5.11 and Figure 5.12). The SDA grid (longest cell side aligned with the channels—perpendicular to the coast) is relatively poor at retaining the shoreface boundary morphology and position but is relatively good at modelling the channel morphology (Figure 5.13). The SSA grid (longest cell side aligned to the coastline) retains the detail of the shoreface boundaries, but is relatively poor at retaining the morphology of the channels (Figure 5.14). Compared to the other grid designs (Figure 5.12 and Figure 5.13)

the cells in the SSA grid exceed the channel width at a lower amount of upscaling—10 times instead of 20 times for the SDA and square grids. At the highest level of upscaling, the channel facies has melded into the background in all models (Figure 5.8 and Figure 5.9). The shoreface has become straight in all models and the width of the shoreface is significantly narrower in the SDA grid than in the square or SSA grids.

5.2.2 Porosity Models

The porosity models were upscaled for all scenarios. The changes in the distribution of porosity in the grids were examined visually and by creating histograms for each grid (Figure 5.15 and Figure 5.16). Both these methods indicate a smoothing out of porosity values as the grids are upscaled.

5.2.2.1 Channel Models

100 m channels

The porosity distributions for the 24-layer 100-25 scenarios all show similar changes in porosity distribution once the cell width exceeds the channel width, irrespective of grid design (Figure 5.16 and *Appendix 3*).

As grids are upscaled vertically the porosity distribution alters, and while remaining bimodal, the two populations become more 'rounded' (Figure 5.17 and Figure 5.18). The average thickness of the cells in the 3-layer grids is slightly larger than the average thickness of the channels. It is likely that, thinner channels are being ‘averaged out’ and blending into the overbank facies in these grids. When grids are upscaled horizontally and vertically at the same time, the horizontal upscaling has a far greater impact on the porosity distribution. Once the cell width exceeds the channel width, the porosity distribution rapidly tends towards a normal distribution (Figure 5.18). The same trends in porosity distribution with horizontal upscaling are also seen in scenarios with 50% gross sand (Figure 5.19 and Figure 5.20).

280 m channels

The porosity distributions for the 280 m channel scenarios are similar to the 100 m channel scenarios, as the porosity distributions for the 280 m scenarios show a shift in porosity distribution once the cell width exceeds the channel width (Figure 5.21, *Appendix 3*). The variogram used to model porosity in the channels in the fluvial models has a width of 100 m and a length of 1000 m. This produces long thin porosity, and subsequently permeability, streaks that follow the orientation of the channel body (Figure 5.22). These porosity streaks are smoothed out in the 280 m channel scenarios before the cell width exceeds the channel width. The porosity histogram shows shifts in porosity distribution, within the bimodal distribution, which may be related to averaging affects within the channels due to upscaling beyond the width of porosity streaks. As with the SQ100-25 scenario, the trends seen in the SQ280-25 scenario are repeated in the SDA and SSA grids and the 50% gross sand scenarios (*Appendix 3*).

5.2.2.2 Shoreface Models

The factors that influence the upscaling of the two shoreface scenarios are the width of the shoreface, the width of the channels and the thickness of the shoreface. The influence of the channels in the shoreface scenarios was studied by comparing the changes to the porosity distributions of both shoreface scenarios (with and without channels). As was shown in *section 5.2.1,* the thickness of the shoreface facies is such, that the facies boundaries are not seriously affected by upscaling until the final level of upscaling (10 x 8 grid) (Figure 5.23).

Vertical upscaling of the beach and coast scenarios induces obvious changes to the porosity distribution over all the grid steps (Figure 5.24 and Figure 5.25). The distribution of low porosity values (<10%) contracts rapidly with vertical upscaling. Although eye-catching, this change in porosity distribution is most likely to affect the offshore and coastal plain facies—neither of which are expected to contribute significantly to field production in these models. With the horizontal upscaling there is no point at which the distribution of porosity suddenly changes as it does in the channel scenarios (Figure 5.24 and Figure 5.25). Rather, the porosity distribution changes gradually, and is most likely to be dominated by averaging

affects within each facies, rather than the redistribution of facies. The bimodal porosity distribution is caused by the distinct differences between the ‘reservoir’ and ‘non-reservoir’ facies (Figure 5.26). In the beach scenario there is no apparent amalgamation of porosity distributions as there is in the channel scenarios. The porosity in the shoreface facies was modelled with a variogram that had its longest axis parallel to the shoreface. This produced areas of high (and low) porosity in large, elongate patches (Figure 5.26). These patches are narrower than the width of the shoreface, and are lost due to the averaging effect long before the boundaries of the shoreface are altered by upscaling. Histograms of the shoreface component of the beach scenario (square grid design) show that the impact of vertical upscaling is most noticeable in the 6 and 3-layer grids for all upscale steps when compared to the 500 x 400 x 24 grid (Figure 5.27). For the 24 and 12-layer grids the porosity distribution closely matches that of the 500 x 400 x 24 grid up to and including the 50 x 40 grid. If horizontal upscaling steps are compared only to the base grid (500 x 400) with the same number of layers then all vertical upscaled grids have a similar porosity distribution to the base grid up to the 50 x 40 grid.

A comparison of the ‘beach’ and ‘coastal’ scenarios indicates that there are slight differences in porosity distribution (Figure 5.28). The channels in the ‘coast’ scenario have an average width of 280 m—the same as the width of the cells in the 50 x 40 grid (square grid) (Figure 5.29). The channels and shoreface facies have similar porosity ranges, but different distributions (Figure 5.30). These differences, along with the differences in size of the facies bodies contribute to them behaving differently during the upscaling process. The porosity histogram for the shoreface facies (24 -layer grid) retains much of its shape up until the final, coarsest grid (Figure 5.31). In contrast, the fluvial facies porosity distribution rapidly loses its low end tail—values less than 12%, and the distribution changes dramatically once the cell width exceeds the channel width (Figure 5.32). These changes in distribution influence the total porosity histogram in a subtle manner (Figure 5.31).

5.2.3 Pore Volumes

The pore volume associated with each facies in each of the geological scenarios was extracted and plotted for realizations one to three. These data indicated that there were only minor differences in pore volumes between different realizations of the same grid design (Figure 5.33). The pore volumes reflect the trends identified in the porosity models (see *section 5.2.2*). The advantage of examining the pore volumes is that multiple realizations can be compared easily and the changes to volumes caused by upscaling can be quantified.

5.2.3.1 Channel Models

Although all scenarios (for each grid design) have the same total pore volume, upscaling produces a change in the distribution of pore volume between facies (Figure 5.37 and Figure 5.38). All scenarios show changes in facies related pore volumes as grid blocks are horizontally upscaled beyond the width of facies bodies (Figure 5.39, and *Appendix 4*). The change is most noticeable in the scenarios with 25% gross sand (Figure 5.39). It is less distinct with 50% gross sand scenarios (Figure 5.40 and Figure 5.41).

The pore volume associated with the facies model decreases as the number of layers in the grids decreases (Figure 5.39 and Figure 5.40). When the width of the cell is less than the width of the channels, the change in pore volume due to vertical upscaling is more significant than the change due to horizontal upscaling (Figure 5.38). However, once the cell width exceeds the channel width, horizontal upscaling has a greater influence on pore volume distribution than vertical upscaling.

5.2.3.2 Shoreface Models

The pore volume associated with each facies in the ‘beach’ scenario does not change with upscaling—vertical or horizontal (Figure 5.34). The cell size never exceeds the width of the shoreface facies, thus minimizing the movement of pore volume away from the shoreface facies. Like the ‘beach’ scenario, there is little difference in pore volumes between different realizations in the ‘coast’ scenario (Figure 5.35). A shift in pore volume associated with the fluvial and coastal plain facies can be seen in the ‘coastal’ scenario (Figure 5.36, *Appendix*

4). The majority of the pore volume associated with the fluvial facies is redistributed into the coastal plain facies. As was seen in the 'channel' scenarios, there is a drop in pore volume associated with the fluvial facies with each stage of vertical upscaling. The mean channel thickness in the 'coast' scenario is the same as the mean cell thickness of the 6-layer grid. The influence of horizontal upscaling on the pore volume of the fluvial facies is similar to that seen in the 'channel' scenarios. The pore volume changes significantly once the cell width exceeds the mean width of the channels (Figure 5.36).

5.2.4 Connected Volumes

The volume of channel facies connected to each of the five wells was also calculated for the square grid. Connectivity is defined as cells of the same facies code which have at least one cell side in common (Roxar, 2006). The results indicate that when the wells in the base model are connected to the channel facies they all see the same volume of sand (Figure 5.42). This shows that for the base model, if the well penetrated a channel, then it is connected to all the fluvial sandbodies. This result was seen for both the 25% gross sand models as well as the 50% gross sand models. As the grids are upscaled the connected volumes remain virtually unchanged until the cell size exceeds half the channel width. At this point, the connected volume drops rapidly and wells begin to see different volumes (Figure 5.43).

5.3 Discussion – Upscaling

5.3.1 Facies Models

The impact of upscaling on a geological model is the reduction of complexity. Although this may be necessary in order to achieve a model that can produce reservoir simulation results in a timely manner, care needs to be taken that the process of upscaling does not remove critical geological features such as high or low permeability streaks and distinct channel boundaries or shoreface interfaces. Any upscaling results in the loss of complexity, however

the data shown indicate that the loss of information can be minimized if grids are designed carefully. The pore volume plots indicate that the total pore volume of the model remains relatively constant at all levels of upscaling; indicating that the software is reliably capturing the overall porosity of the base model. However, the data clearly show that there is a shift in porosity distribution and consequently pore volumes associated with facies when cells sizes exceed half the width of the sandbodies. Once the cells are larger than the sandbodies, the petrophysical properties of the model rapidly tend towards a normal distribution, no matter what the distribution of original data is.

Upscaling beyond half the width of the sandbodies can alter the sizes and connectivity of the bodies; potentially making them significantly larger than desired, or losing them all together. An example of this would be a tidal channel cutting through a barrier-island shoreface (Figure 5.45). As the permeability profiles in tidal channels may be the opposite of the surrounding shoreface sediments (upward- fining vs. upward-coarsening) this averaging effect at large cell sizes has the potential to smooth out the permeability profile of the reservoir, giving a distorted, less complex view of flow through the flow unit.

Upscaling of shorefaces has the potential to alter the position of the shoreface boundaries. The location of boundaries with significant porosity/permeability contrasts such as the upper/lower shoreface interface has been shown by (Kjønsvik et al., 1994) to have a major influence on water flood performance. Careful grid design can minimize the amount of variation induced during the upscaling process (Figure 5.9). The porosity distribution of the coast and beach models appears to have greater change when upscaled vertically than horizontally (Figure 5.27). Although the 24 and 12 -layer grids provide the best match of porosity distribution, if the 6 or 3-layer grids are used, then they can be upscaled horizontally to the 50 x 40 grid step before the porosity distribution will be significantly different from that of finer grids with the same number of layers.

5.3.2 Porosity

All the porosity distributions presented indicate that once the cell size exceeds the channel width, the contrast between channel and overbank begins to disappear and the porosity distribution tends towards a normal distribution. Comparison of the 100 m channels and the 280 m channels indicate that the channel morphology vanishes at between 1 and 2 times the channel width (Figure 5.15 and Figure 5.21). Once the channel width is exceeded, the high porosity streaks of the channels become less continuous and blurred in plan view. The histograms of porosity distribution become rounded when channel width is 1-1.5x cell width, and the bimodal distribution is lost at approximately 2x cell width. As the grids are upscaled vertically the porosity distribution becomes truncated (Figure 5.17 and Figure 5.18—500 x 400 grid). As the channel thickness is never exceeded by the cell thickness, vertical upscaling does not result in loss of the bimodal distribution in this dataset. It is anticipated that further vertical upscaling would see a shift to a normal distribution.

5.3.3 Connected Volumes

While it was expected that the 50% gross sand models would be well connected, prior to building the model the 25% gross sand models were not expected to be well connected. Published data, such as King (1990), Ainsworth (2005), Larue and Friedmann (2005) and Larue and Hovadik (2006) suggests that a net sand content of less than 30% is likely to produce poorly connected channels. Historical descriptions of connectivity that placed the net:gross ratio required for extensive connectivity at 40–50% appear to have been calculated either using a 2D dataset (Allen, 1978) or straight channels with similar orientations (Henriquez et al., 1990). The higher than anticipated amount of channel connectivity in the 25% gross sand scenarios is most likely the result of the channel design used in this project. The sinuosity of the channels, in combination with the amount of variability of channel orientation is enough to produce a higher level of connectivity than anticipated (Figure 5.46). The channel connectivity is such that, in most realizations, any well penetrating the channel facies is connected to all the channel facies. Channel connectivity drops as the grids are upscaled beyond half the width of the channels.

5.4 Conclusions – Upscaling

The following points should be considered when designing base geological models and any models for reservoir simulation:

- Width of cells should be no more than half the width of the reservoir sandbodies. Upscaling beyond half the width of the channel (or other facies) will result in loss of morphology (Figure 5.21),
- Thickness of layers should be less than half the thickness of individual bodies,
- Shape and orientation of cells should reflect the orientation of the major sandbodies. Square cells are the best way to minimize morphology problems that can result from upscaling (Figure 5.7),
- Upscaling has the potential to change flow paths. Upscaling beyond the width and/or thickness of thin features (porosity/permeability zones or barriers) will result in their loss —which may introduce, remove or smooth flow paths (Figure 5.45),
- A simple visual test can be used to assess how well the upscaled grid has captured the data. If the geological features cannot be recognised by looking at a layer in the upscaled grid, the properties of the upscaled grid are unlikely to be similar to those of the original grid (Figure 5.31).

5.5 Figures – Upscaling

Grid Design	Rows	Columns	Multiplier	mX	mY	Number of Cells			
						24 layers	12 layers	6 layers	3 layers
Shoreface Strike Aligned	**600**	**800**	1	24	12	6,905,352			
	300	**400**	2	47	24	1,728,312	864,156	432,078	216,039
	150	**200**	4	94	49	432,984	216,492	108,246	54,123
	120	**160**	5	118	61	277,296	138,648	69,324	34,662
	60	**80**	10	235	123	69,600	34,800	17,400	8,700
	30	**40**	20	471	246	17,496	8,748	4,374	2,187
	15	**20**	40	942	491	4,392	2,196	1,098	549
	12	**16**	50	1177	614	2,784	1,392	696	348
	6	**8**	100	2354	1228	648	324	162	81
Square	**1000**	**800**	1	12	14	11,502,984			
	500	**400**	2	28	24	2,877,768	1,438,884	719,442	359,721
	250	**200**	4	56	48	720,384	360,192	180,096	90,048
	200	**160**	5	70	60	461,256	230,628	115,314	57,657
	100	**80**	10	140	120	115,632	57,816	28,908	14,454
	50	**40**	20	280	240	28,872	14,436	7,218	3,609
	25	**20**	40	560	480	7,320	3,660	1,830	915
	20	**16**	50	700	600	4,656	2,328	1,164	582
	10	**8**	100	1200	1400	1,128	564	282	141
Shoreface Dip Aligned	**1200**	**400**	1	12	25	6,910,752			
	600	**200**	2	24	50	1,730,904	864,156	432,078	216,363
	300	**100**	4	47	98	433,872	216,936	108,468	54,234
	240	**80**	5	59	123	278,064	139,032	69,516	34,758
	120	**40**	10	118	246	69,972	34,896	17,448	8,724
	60	**20**	20	325	491	17,544	8,772	4,386	2,193
	30	**10**	40	471	982	4,392	2,196	1,098	549
	24	**8**	50	588	1228	2,784	1,392	696	348
	12	**4**	100	1177	2456	696	348	174	87

Figure 5.1. Matrices showing the grid designs built and how they were upscaled. The blue shading highlights the grids that reservoir simulation was carried out for. The darker blue shading highlights the grids for which simulation was carried out on ten realizations. Only three realizations were simulated for the 24, 12 and 6-layer grids.

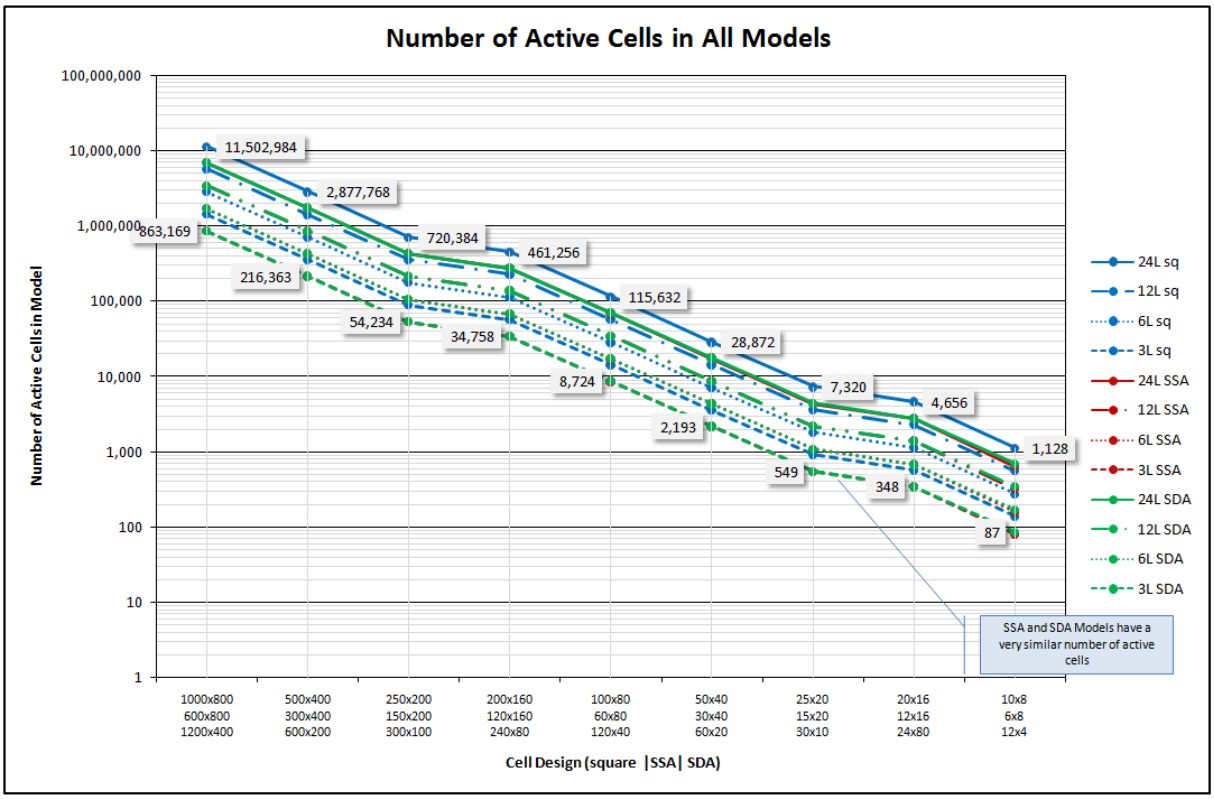

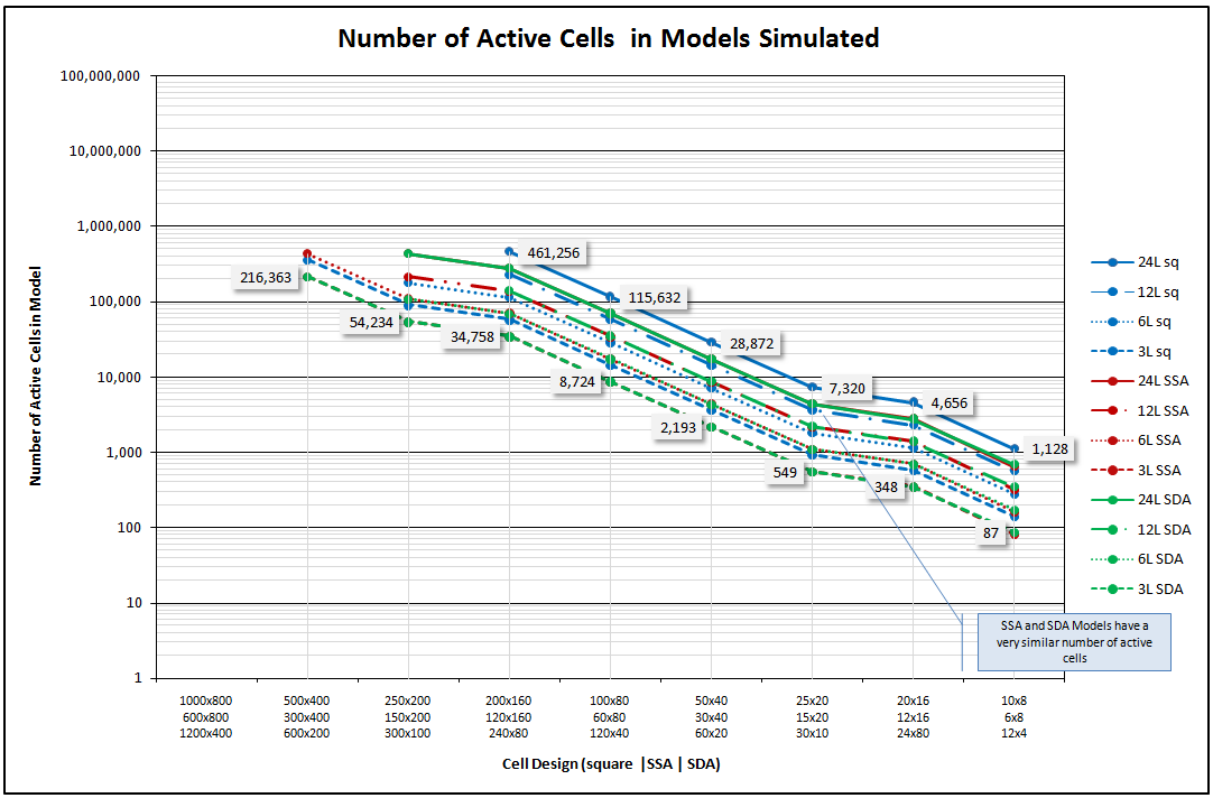

Figure 5.2. Number of active cells in the models built. The horizontal axis (Grid Design) refers to the horizontal upscaling steps. The vertical upscaling is represented by the L on the data title. For example, 24L SSA = 24 layers, SSA grid; 12L sq = 12 layers, square grid and 6L SDA = 6 layers SDA grid. Graph A shows the number of cells in all the model designs built. This shows that the base geological models have between 10 and 11 million cells in them. With the technology available in this project, these grids were too large for reservoir simulation. The SSA and SDA grids have the same number of cells at each upscaling step. Graph B shows the number of active cells in the grids for which reservoir simulation was carried out. An upper limit of approximately 450,000 cells was applied in this project. Grids of this size could take up to a week for a simulation run.

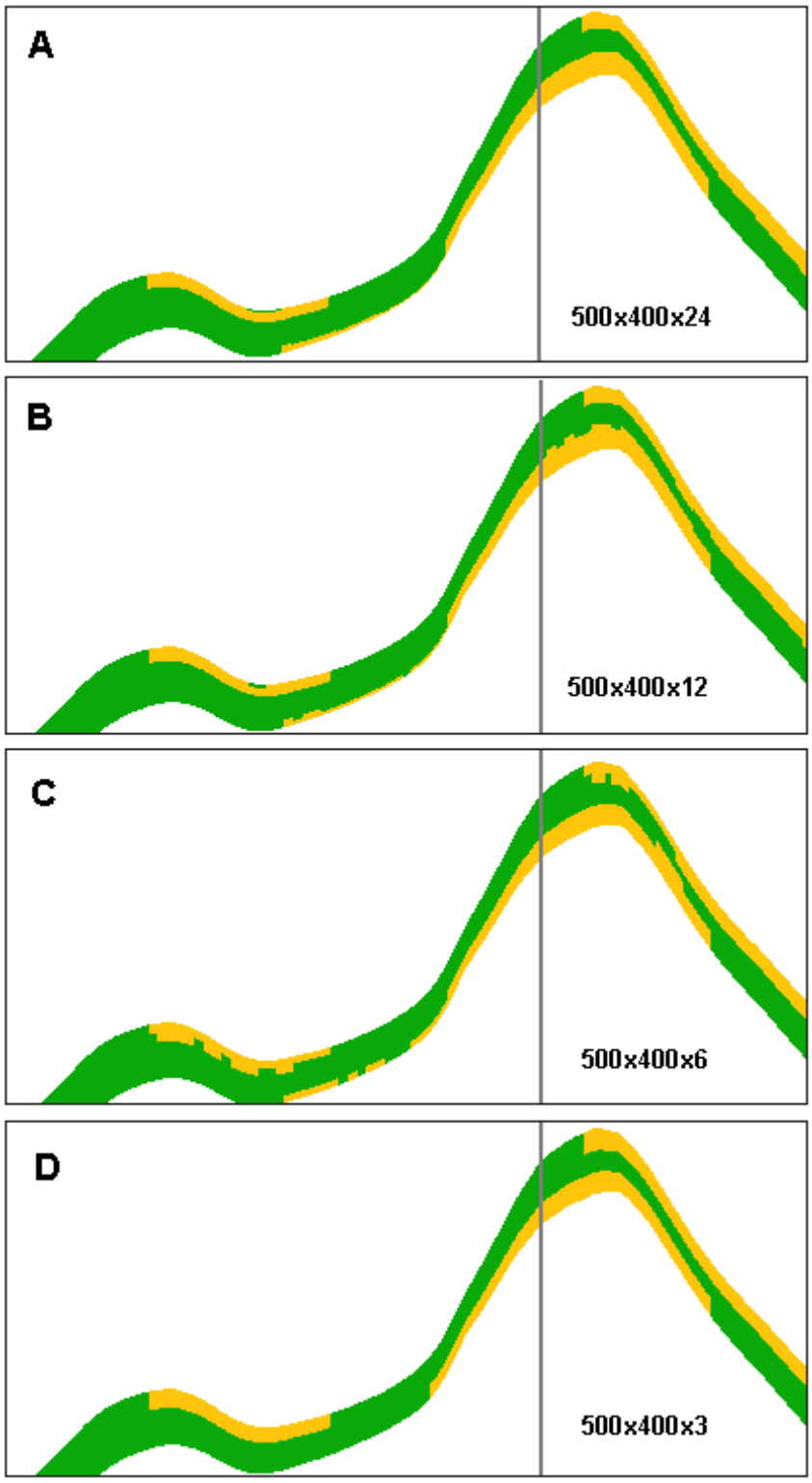

Figure 5.3. Vertical upscaling of channels. The channels in this model (SQ 280-25) are upscaled vertically but not horizontally. It can be seen that although the thin channels are merged into the overbank facies, the average thickness channels remain similar to their original form.

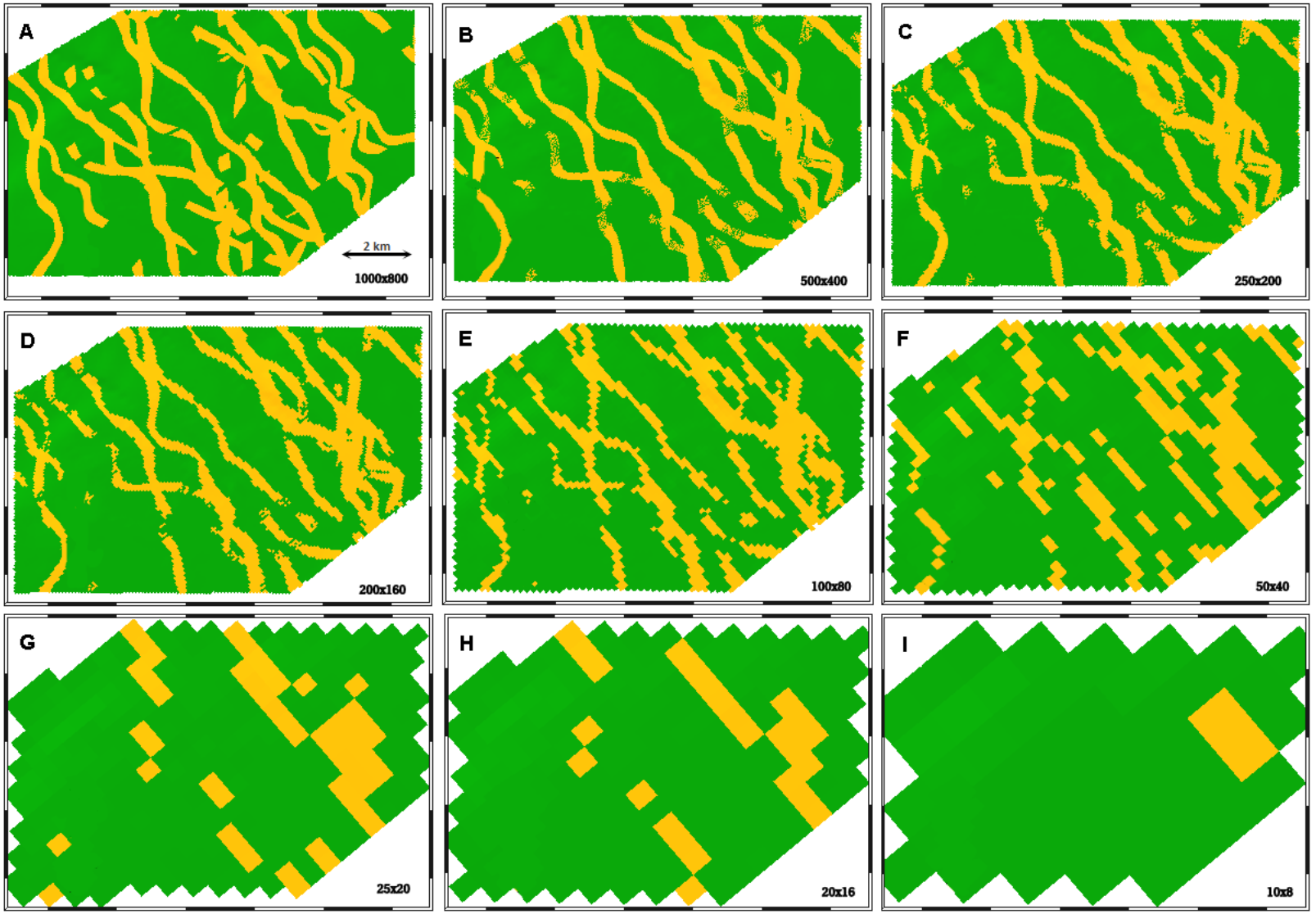

Figure 5.4. SQ280-25 scenario, 24 layers. The average channel width is the same width as the cells in the 50 x 40 grid (F). Upscaling to this level results in the loss of channel morphology and connectivity. The channel width is twice that of the cell width in the 100 x 80 grid (E). At this point channel morphology and connectivity is preserved. Once the cell size is more than half the average channel width, morphology and connectivity begin to be lost.

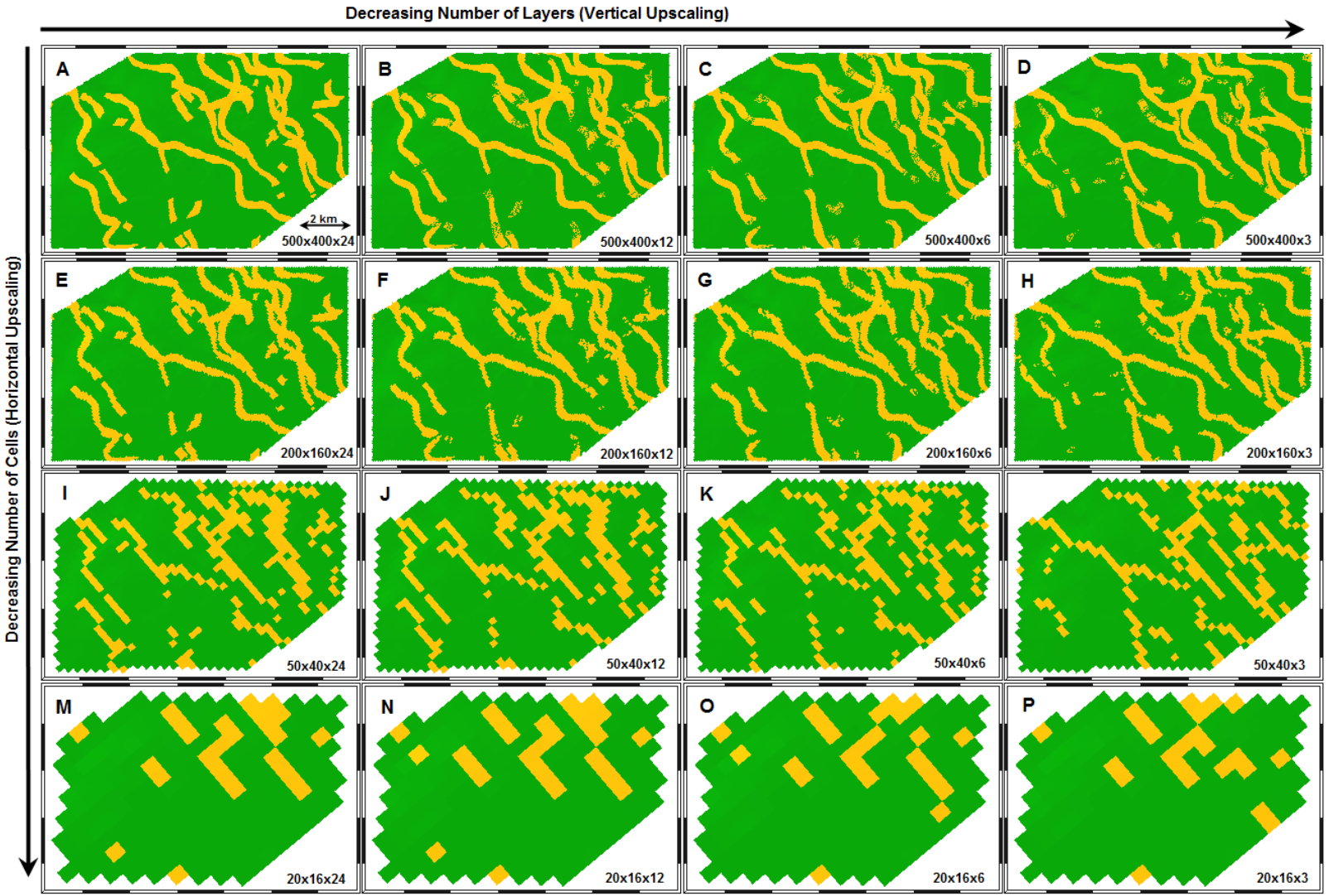

Figure 5.5. Vertical and horizontal upscaling of selected grids. SQ280-25 scenario. The average channel width is the same as the cell width in the 50 x 40 grids (I,J,K,L). When the cell width equals the channel width, connectivity between cells of the same facies becomes restricted to cell corners only in many cases. Vertical upscaling results in relatively minor changes to channel distribution.

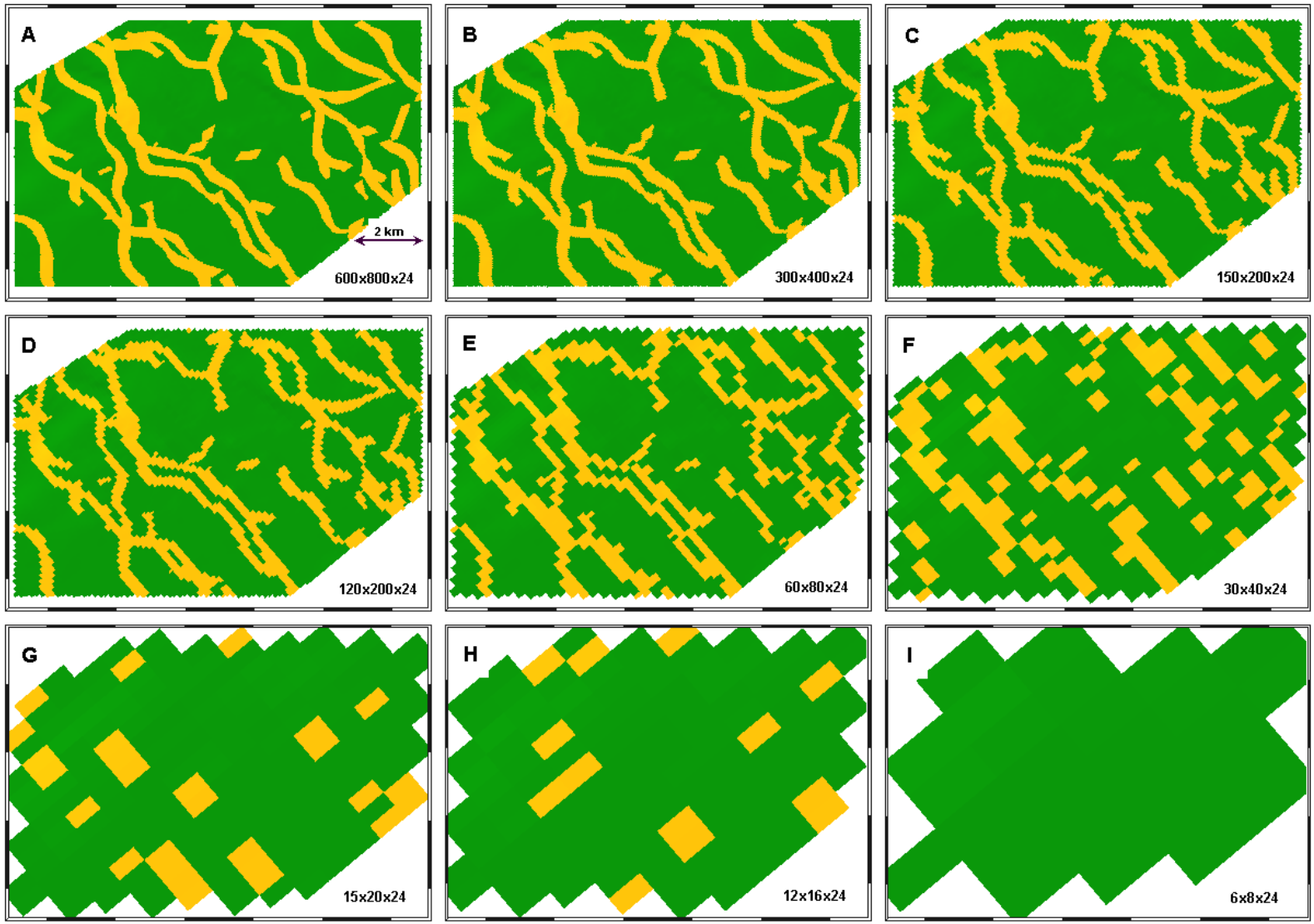

Figure 5.6. SSA280-25 scenario, 24 layers. The average channel width is slightly larger than the cell width in the 60 x 80 x 24 grid (E), and is exceeded in the 30 x 40 x 24 grid (F). Because the channels are oriented approximately perpendicular to the long axis of the cells, the channels in diagram E look much 'blockier' than those in the equivalent grid (F) in the square grid (Figure 5.4) and the SDA grid (Figure 5.7).

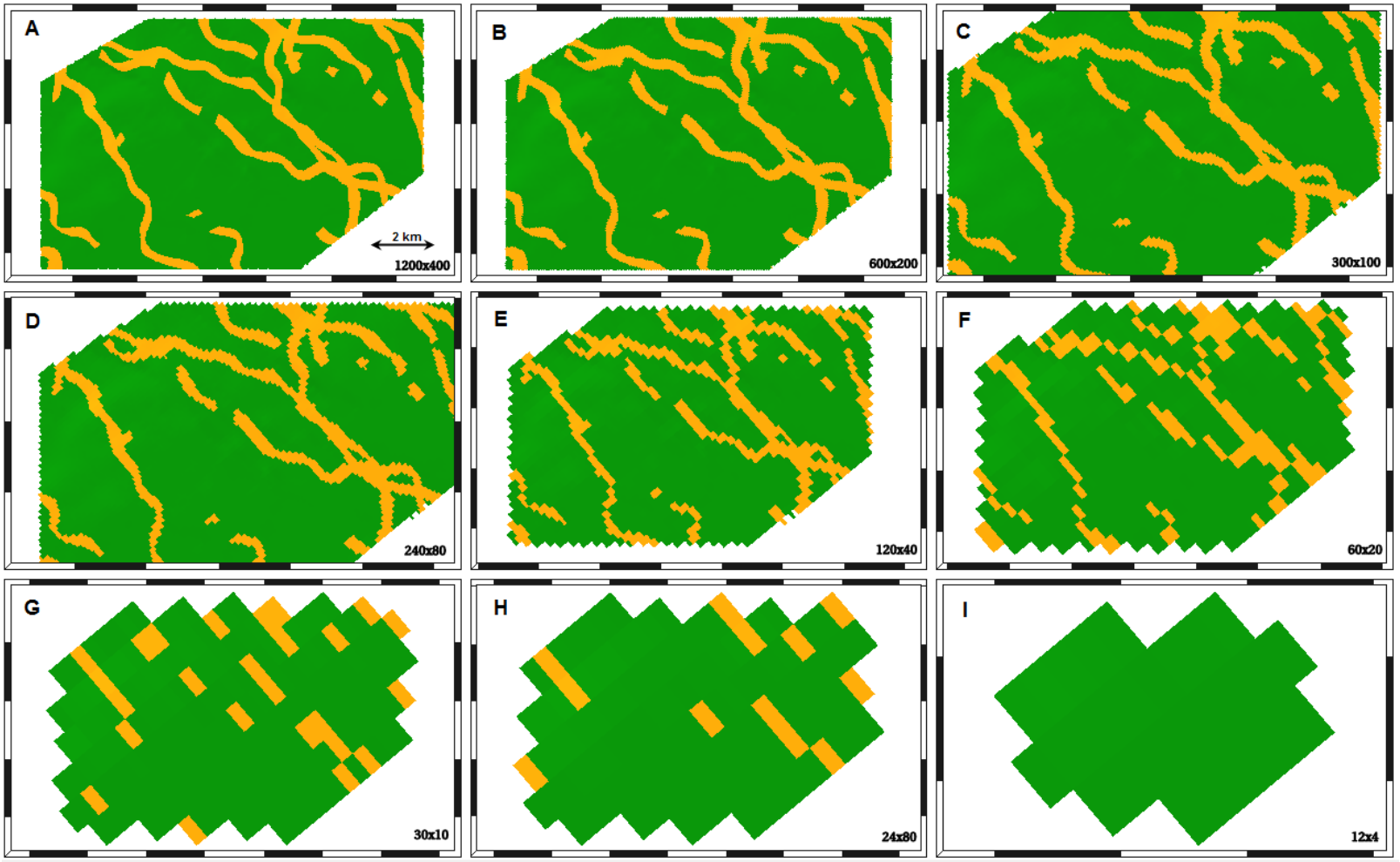

Figure 5.7. SDA280-25 scenario. The average channel width is slightly larger than the cell size in the 60 x 20 x 24 grid (F).

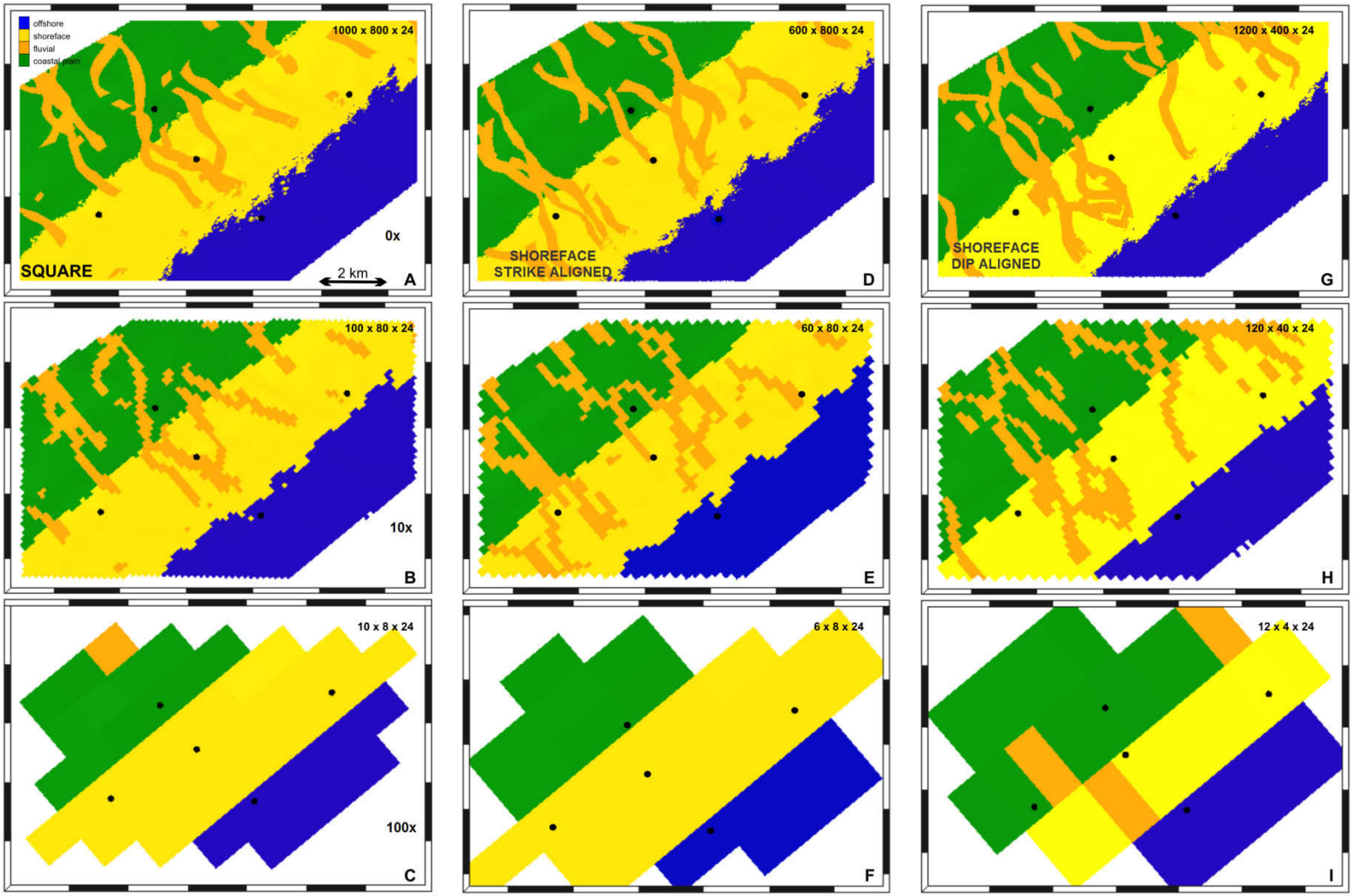

Figure 5.8. Conceptual coastal model. A comparison of the influence on grid design on the upscaling of facies models. The three grid designs produce models that look similar when the cells are small. As the grid cells become larger, the shape of the grids begins to influence the morphology of the channels and the boundaries of facies. At very large grid cells size, the shape of the cells has the potential to significantly change the width of even large features such as shorefaces.

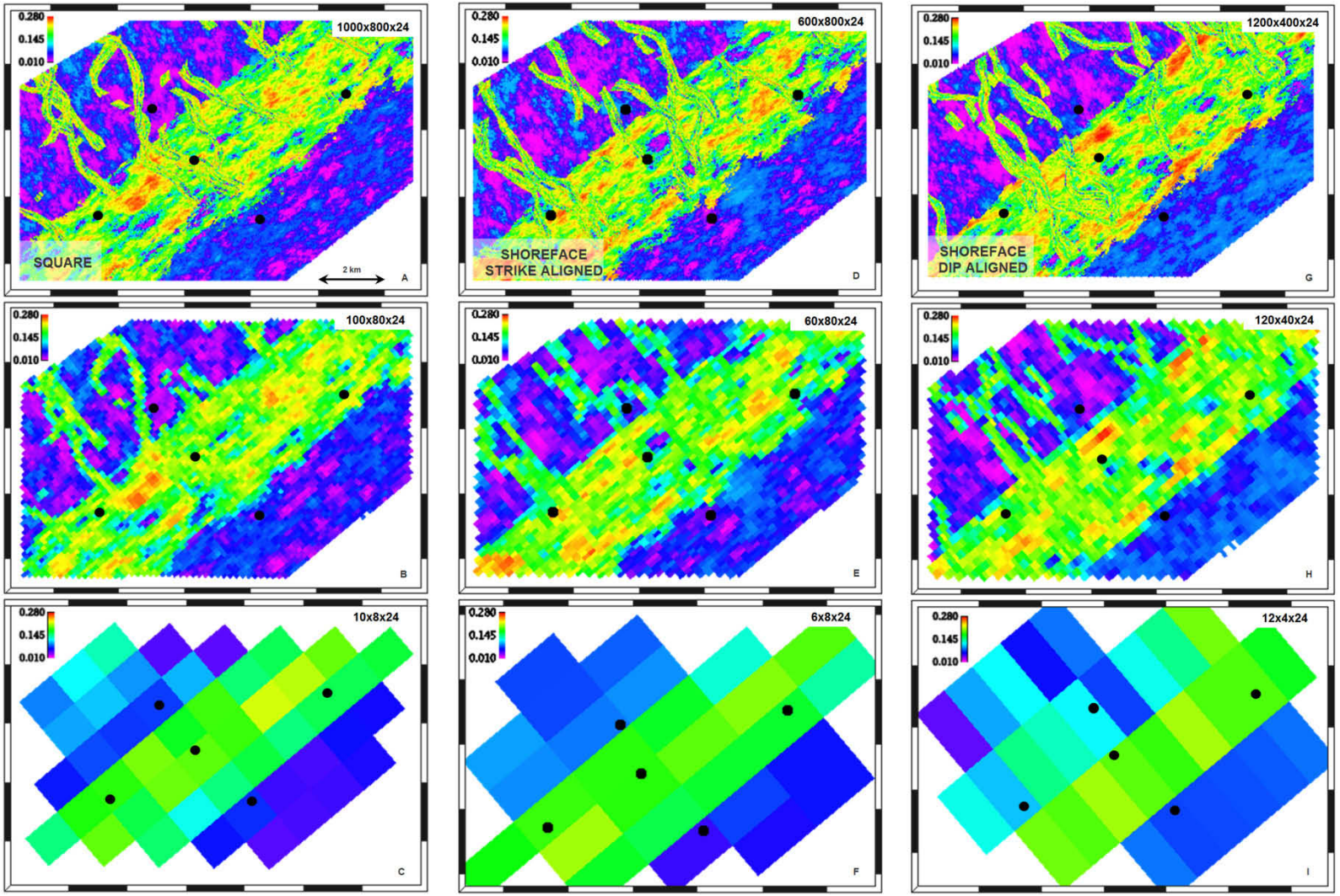

Figure 5.9. The influence of grid cell shape on the upscaling of porosity models. Coastal scenarios, Layer 1. The shape of the grids can have a significant influence on the preservation of porosity sweet spots. The porosity trend in the shoreface facies is parallel to the coast. The square and SSA grids better preserve the porosity sweet spots (red) than the SDA grid. The SDA grid also poorly preserves the width of the shoreface at high levels of upscaling, and this is clearly reflected in the porosity model.

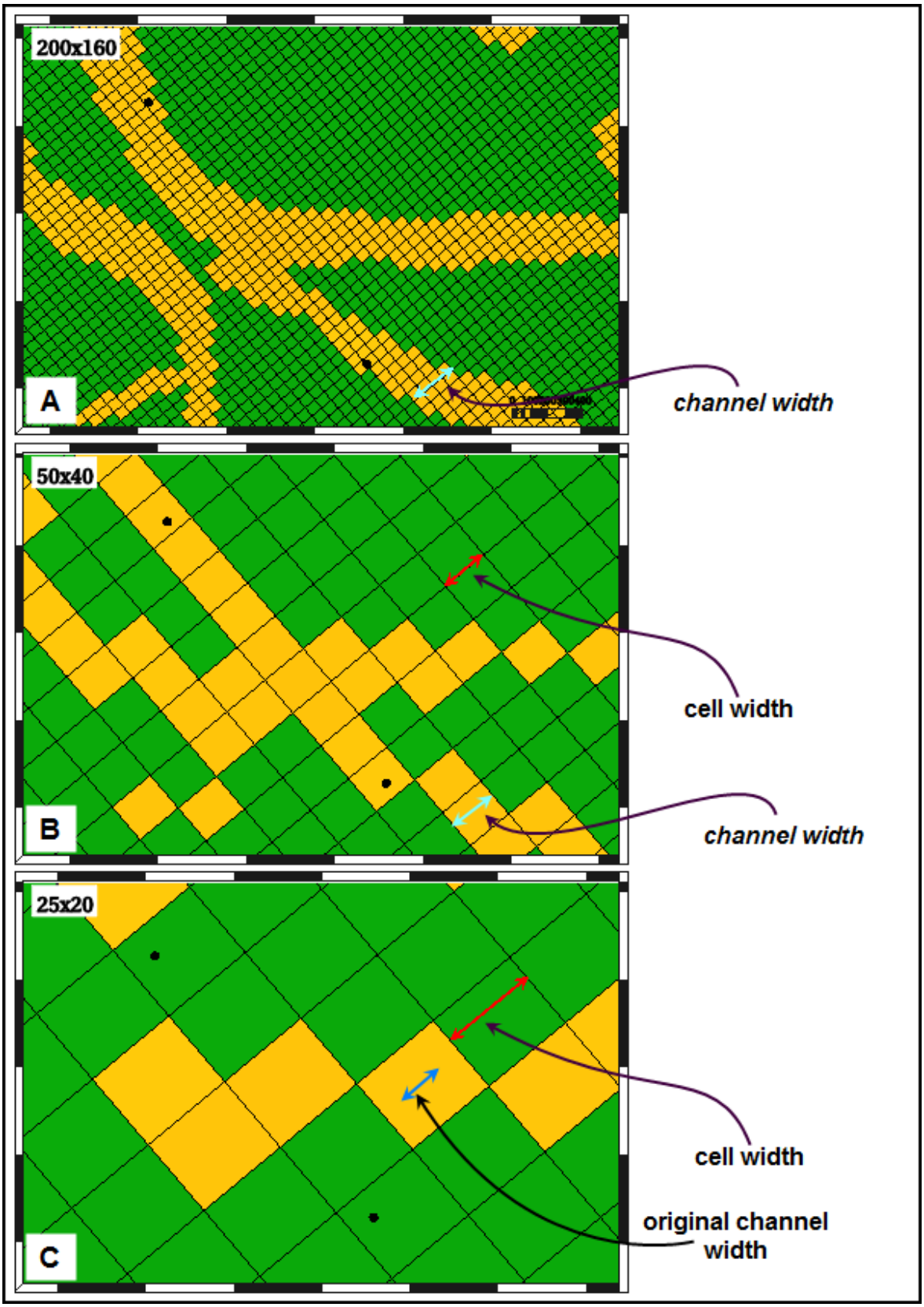

Figure 5.10. The relationship between cell width and channel width. Cell width denotes the width of the cell along the x-axis (red arrows). The width of the channel is the average with of the channel facies (blue arrows). In diagram A, the cell width is less than the channel width. In diagram B the cell width equals the channel width, and in diagram C the cell width exceeds the channel width.

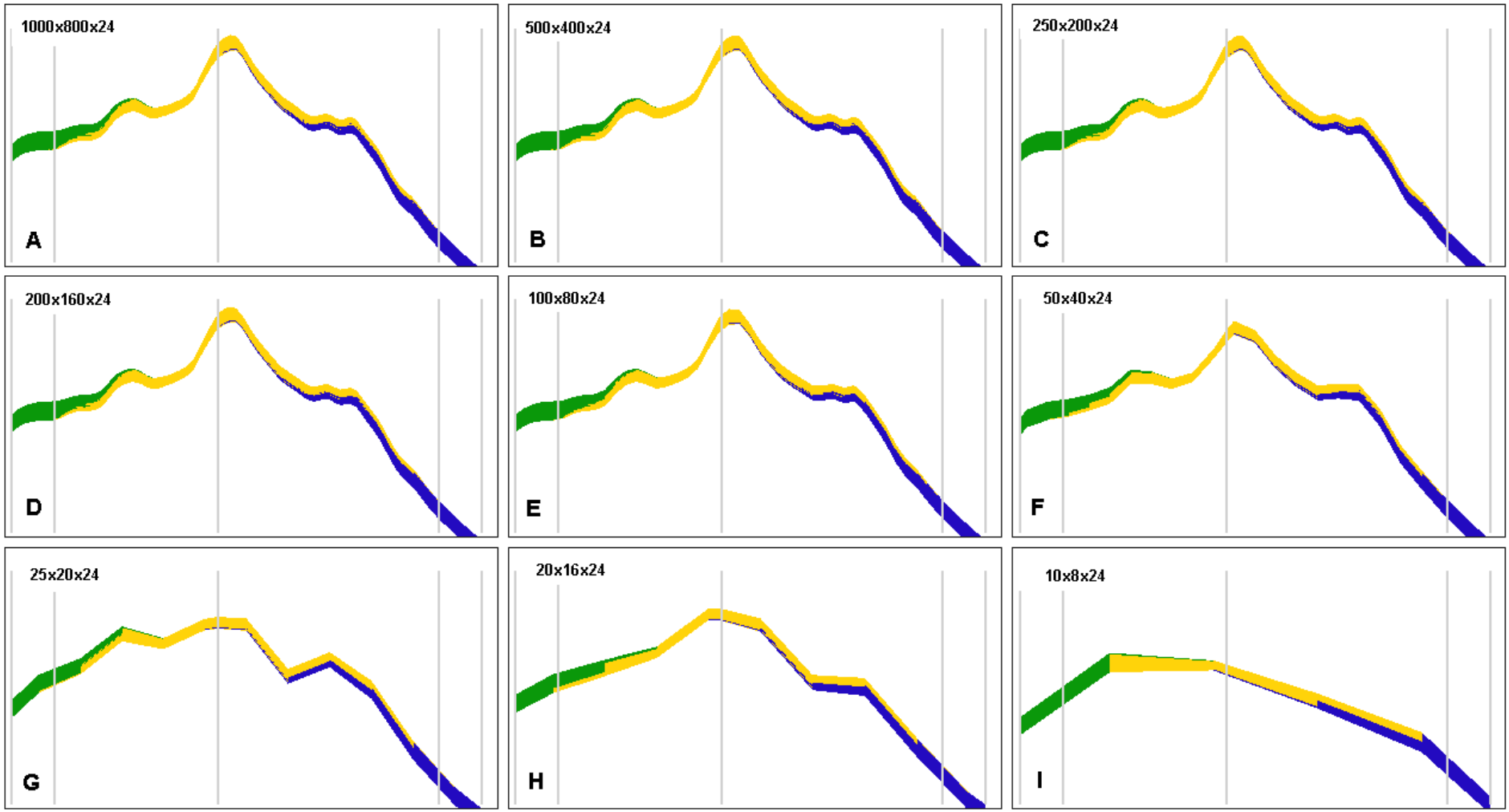

Figure 5.11. Horizontal upscaling of beach model—24-layer grid. The shoreface interfaces become obviously affected by horizontal upscaling in the 25 x 20 grid (I). However, it is not until the maximum level of upscaling (10 x 8) that the shoreface boundaries become significantly different from the original model. Note: the grey lines are hinges on the fence. This diagram also highlights the loss of structural detail that occurs as grids are upscaled (all fences have the same vertical scale and range).

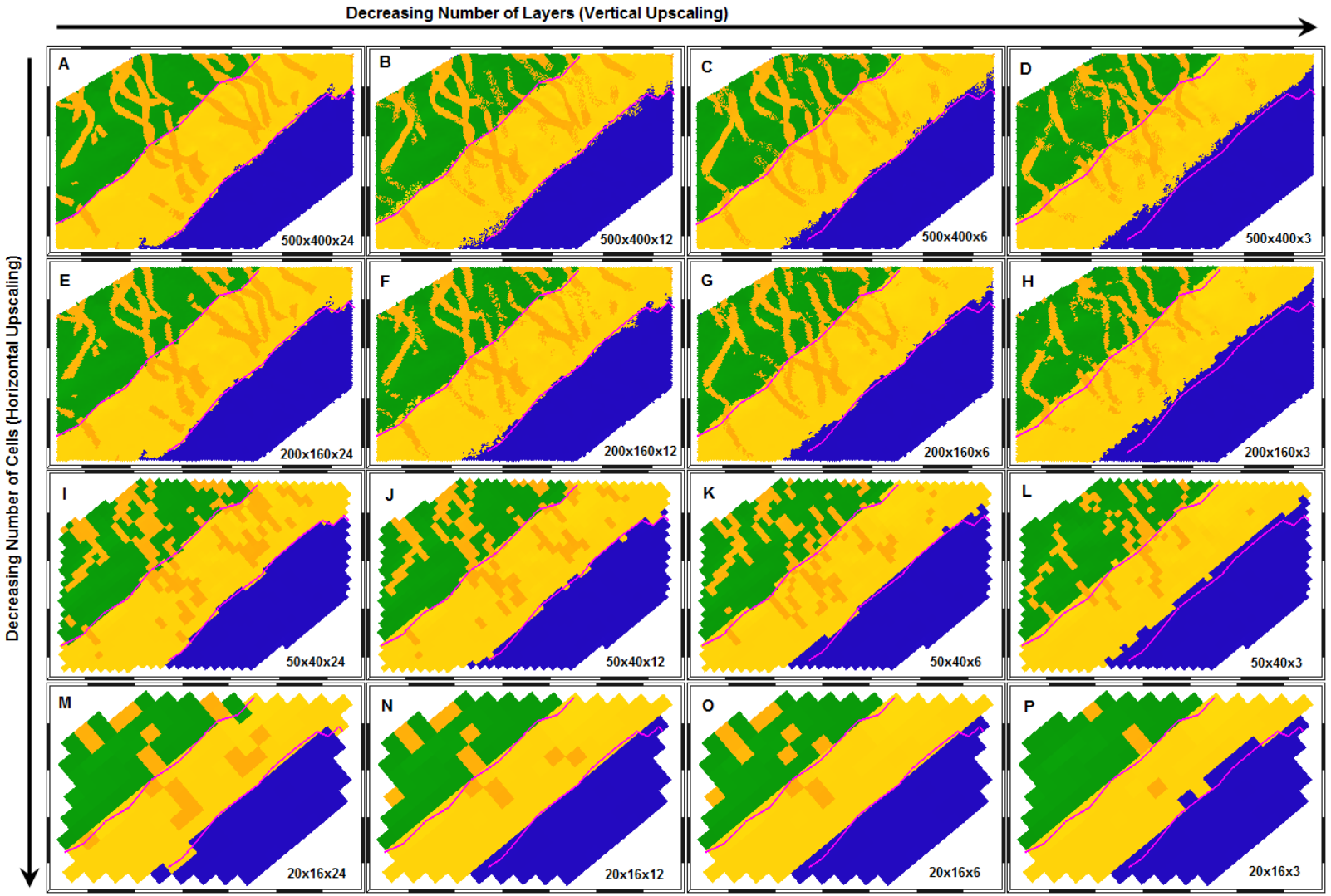

Figure 5.12. Vertical upscaling of the coast scenario—square grid. Selected grids highlight the influence of vertical upscaling on the position of the shoreface and the preservation of the fluvial facies. The mean width of the channels is the same as the cell width in the 50 x 40 grids (I,J,K & L). The pink lines indicate the shoreface boundaries in the base model (A), and highlight how the morphology and position of the facies edge changes with upscaling.

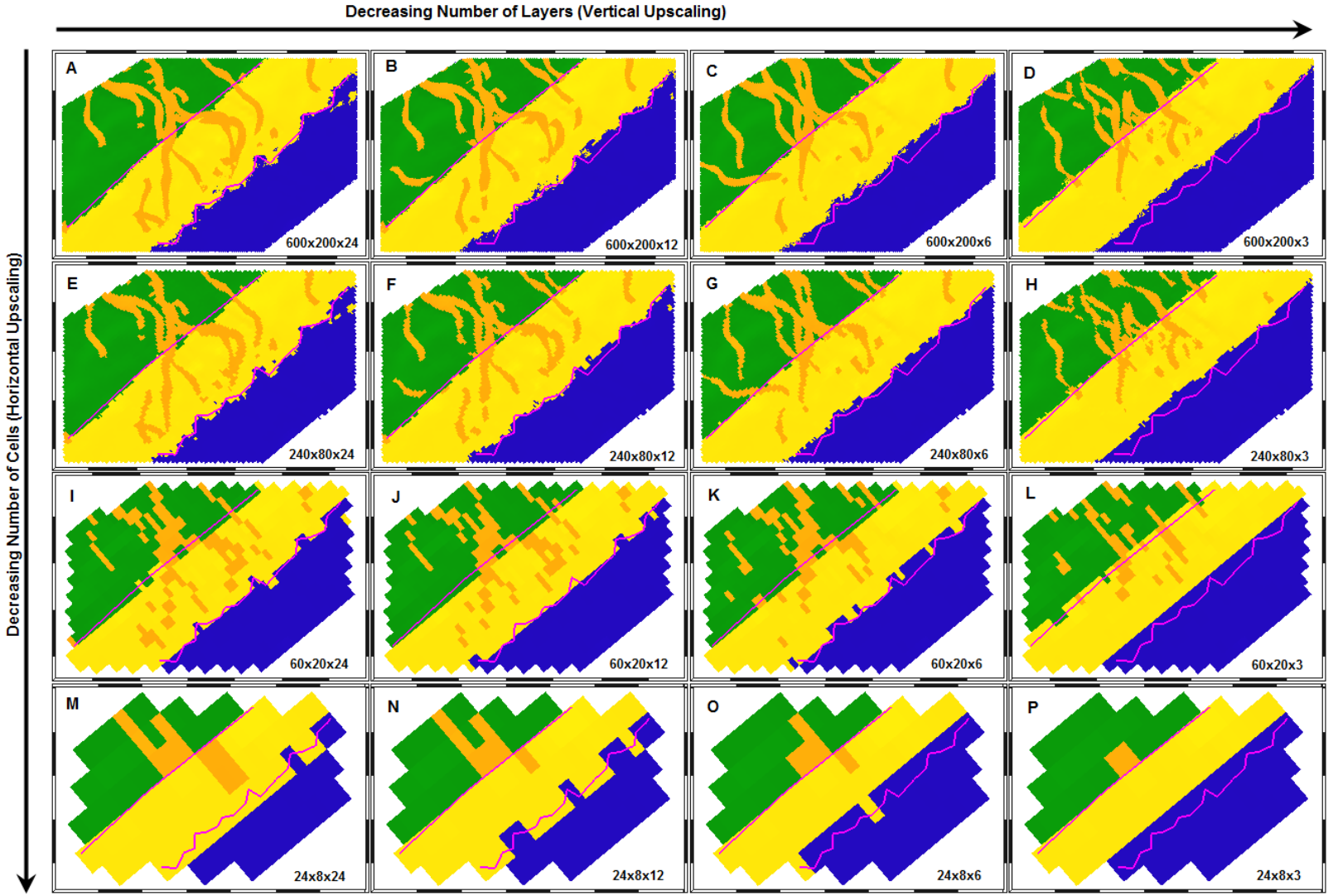

Figure 5.13. Vertical upscaling of the coast scenario—SDA grid. The mean width of the channels is slightly less than the cell width of the 60 x 20 grids (I,J,K & L). This grid design provides better continuity of the channel facies in the equivalent grids than the square grid (Figure 5.12: I, J, K & L). However, it provides poorer preservation of the shoreface boundaries.

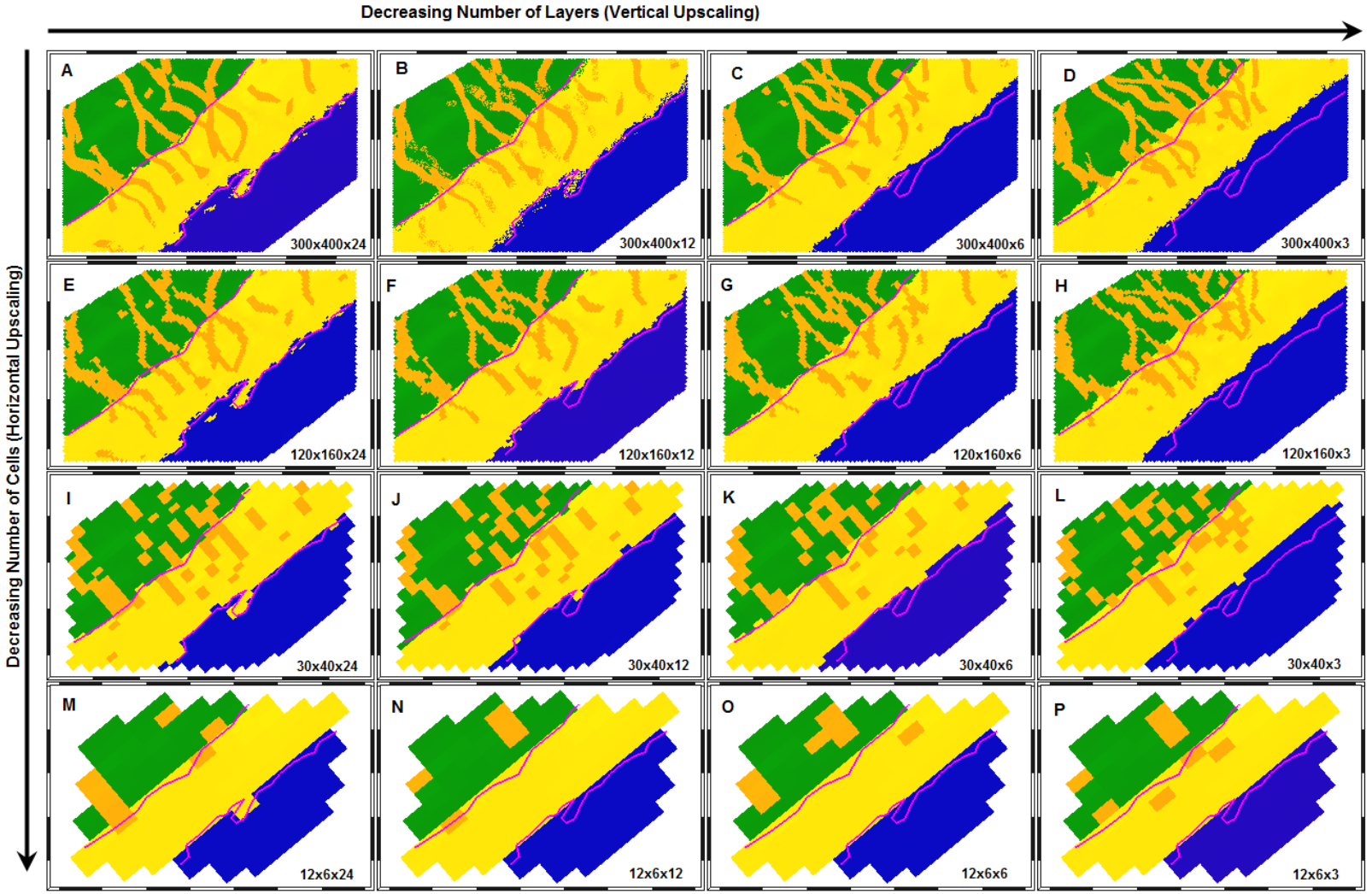

Figure 5.14. vertical upscaling of the coast scenario—SSA grid. In this grid design the channel width is exceeded in the upscale step between the 120 x 160 and 30 x 40 grids. The cell width in the 30 x 40 grids is approximately 1.5 times the channel width.

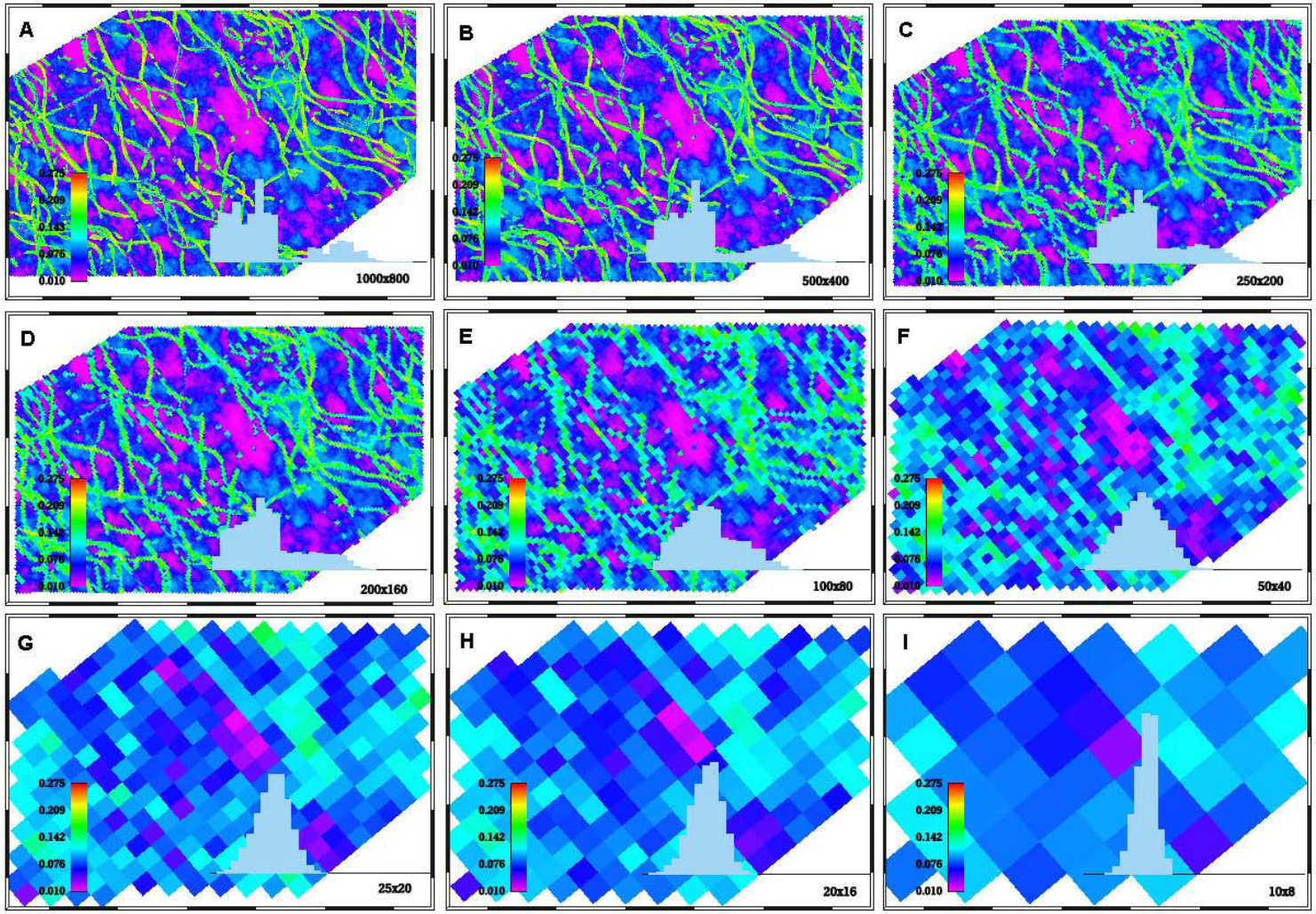

Figure 5.15. Porosity model of a conceptual fluvial channel model. SQ100-25 scenario, 24 layers (layer 1 shown). The base model is diagram A. Channel width is slightly larger than the cell width in diagram D. Although the channels can still be seen in diagram E (cell width is approximately 1.5 times channel width) the morphology of the channels is changing, and thin channels are disappearing. The overbank area contains porosity values up to ten percent (a cut-off was applied) in crevasse splays. The patchy distribution of the porosity (blue) aims to introduce the sporadic nature of crevasse splay reservoir quality rock. The blue silhouette is the porosity distribution for the entire model.

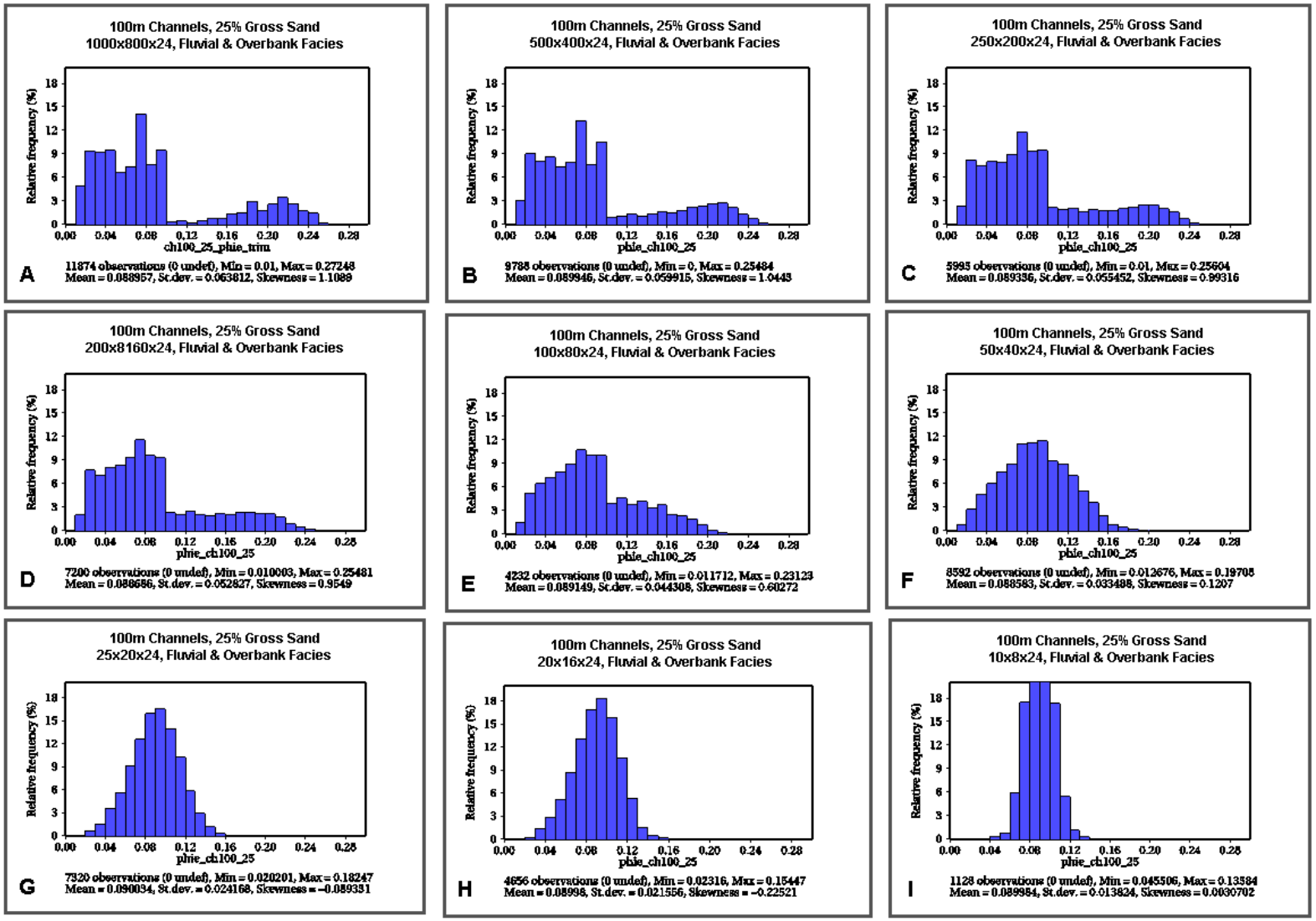

Figure 5.16. Histogram of porosity values for grids shown in Figure 5.15. SQ100-25 scenario. Cell width exceeds channel width between diagrams D and E. In diagram E (cell size is nearly 1.5 times the channel width) the bimodal nature of the porosity distribution is beginning to be lost. It has gone altogether by the time the cell size reaches nearly three times the channel width in diagram F.

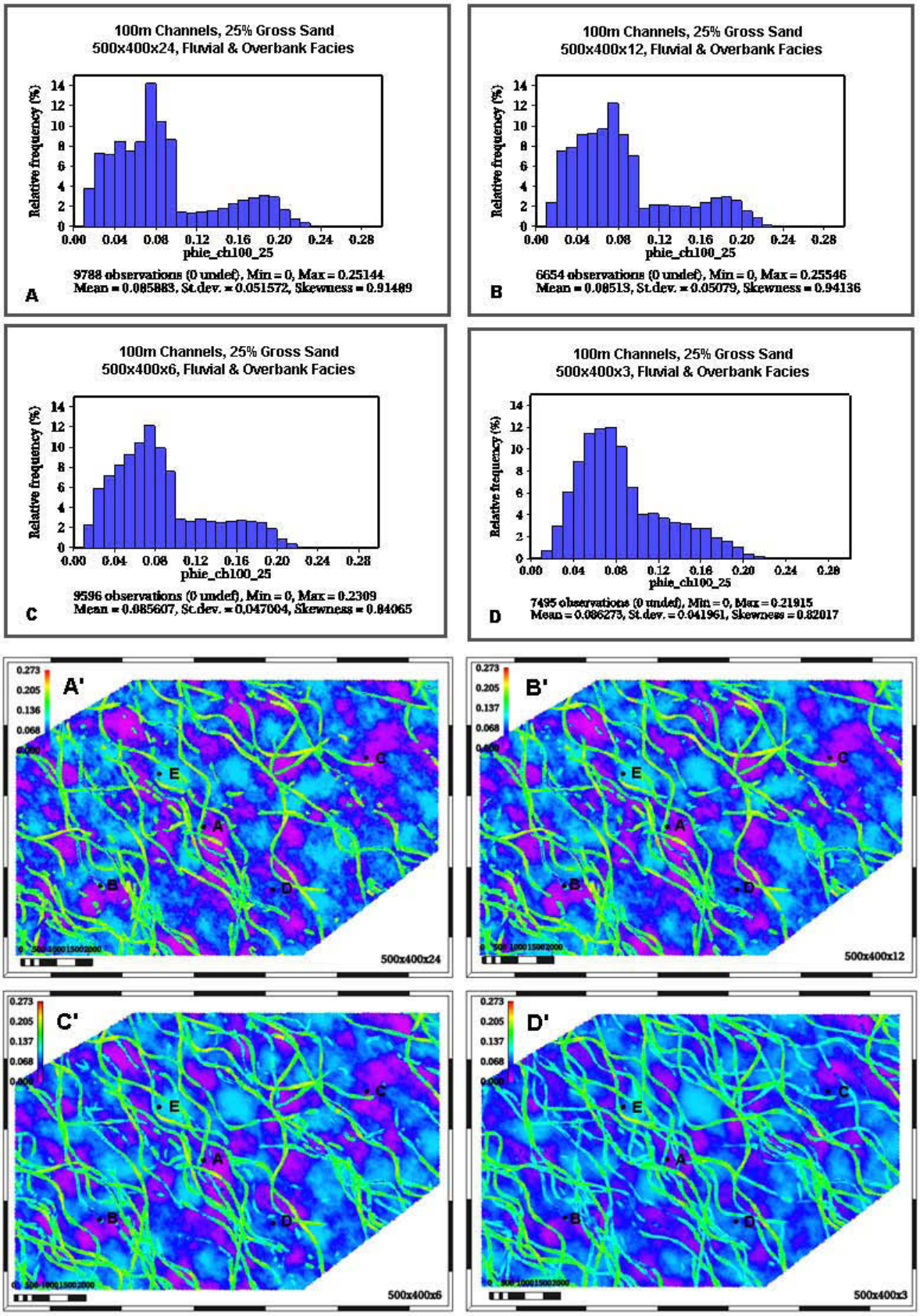

Figure 5.17. Changing porosity distribution with vertical upscaling—square grid. The histograms highlight the changes in porosity distribution as the grids are upscaled. The porosity grids highlight the amalgamation of channels as layers are blended together. All four porosity grids have the same colour scale, which highlights the loss of very low porosity areas (purple). The loss of high porosity streaks is harder to see in the narrow channels. The histograms indicate that the maximum porosity has gone from 25.14% in the 500 x 400 x 24 grid (A) to 21.9% in the 500 x 400 x 3 (D) model.